

PCR inhibition by reverse transcriptase leads to an overestimation of amplification efficiency

Oleg Suslov and Dennis A. Steindler*

McKnight Brain Institute of the University of Florida, FL, USA

Received June 30, 2005; Revised September 19, 2005; Accepted October 25, 2005

ABSTRACT

This study addresses the problem of PCR inhibition by reverse transcriptase. It has been shown that the inhibition occurs mostly when a small amount of RNA is taken for RT reaction, and it is more visible for rarely expressed transcripts. We show here that the inhibition takes place regardless of what amount of template is utilized for RT. The inhibition possesses a global nature, i.e. the amplification of any given transcript may be compromised with different levels of inhibition. The process of inhibition also explains wrongfully derived PCR amplification efficiencies, sometimes more than 100%, when the sequential dilutions of unpurified RT sample are utilized to build the calibration curve. The RT influences PCR not only by inhibiting it. When microgram(s) of RNA are taken for RT reaction, reverse transcriptase may cause overamplification of some transcripts under certain PCR conditions. The possible mechanism of RT influence on PCR is presented, and a purification method is implemented to remove the effects of RT on PCR.

INTRODUCTION

Messenger RNA profiling relies heavily on a reverse transcription step which is accompanied by PCR. The recombinant Moloney murine leukemia virus reverse transcriptase (RT), RNase H deficient (MMLV, H⁻) and avian myeloblastosis virus RT, RNase H deficient (AMV, H⁻) are the most frequently used reverse transcriptases for this purpose. There is a well-known inhibitory effect on PCR by RT components (1–5). The introduction of micrograms of RNA into the RT step, followed by the extensive dilution of RT reaction before PCR execution, is supposed to minimize this inhibition (1,3,4,6,7). These conditions often are not met for two reasons: (i) there is not enough RNA available, and (ii) the extensive

dilution will negatively affect the precise detection of rarely expressed genes. There are other approaches to reduce the RT impact on PCR:

- (i) heating the RT reaction before PCR (3);
- (ii) introduction of T4 gene 32 protein (4);
- (iii) including of non-homologous RNA as a carrier (1);
- (iv) adding of foreign DNA (2);
- (v) excluding DDT from the RT reaction (8);
- (vi) ethanol precipitating RT reaction (5); and
- (vii) phenol extraction followed by alcohol precipitation of RT reaction (3).

The majority of studies of RT inhibitory effects, up until now, were performed using regular PCR. In the present study, utilizing an organic extraction followed by ethanol precipitation of the RT reaction, and a real-time PCR approach, we were able to perform a calculation of an approximate percentage of inhibition in every dilution point of its unpurified counterpart RT reaction. A novel observation here is that a derived PCR amplification efficiency of an unpurified sample may be incorrectly assigned because of the effects of RT on PCR. It is deemed important to remove reverse transcriptase before performing PCR.

MATERIALS AND METHODS

Total RNA isolation

Total RNA was extracted from LN229 primary human glioma cells, grown on six plates (50–70% of confluent) using the RNeasy Mini Kit (Qiagen) with DNase I treatment on the column. Eluted RNA was subjected to a second DNase I treatment in solution using Turbo DNA-free (Ambion). After the treatment, total RNA was cleaned and concentrated using phenol/chloroform/isoamyl alcohol (25:24:1), pH 5.2 (Amresco) followed by ethanol (EtOH) precipitation. Total RNA was dissolved in RNase-free water (Ambion), and the quality was confirmed using an HP 2100 Bioanalyzer (Agilent Technologies). The readings gave a RIN (RNA Integrity Number) value of 9. The isolated RNA had an A_{260}/A_{280} ratio of 2.

*To whom correspondence should be addressed. Tel: +1 352 392 0490; Fax: +1 352 846 0185; Email: Steindler@mbi.ufl.edu
Correspondence may also be addressed to Oleg Suslov. Tel: +1 352 392 6754; Fax: +1 352 392 0025; Email: osuslov@yahoo.com

The lack of phenol contamination was confirmed by measuring the absorbance at 270 and 275 nm using the UV spectrophotometer, SmartSpec 3000 (BioRad).

DNA standards creation

Full-length transcripts of human beta-2-microglobulin (B2M) and TATA box binding protein (TBP) were amplified by PCR using proof-reading Platinum *Taq* DNA Polymerase HiFi (Invitrogen). Polyadenylated mRNA fragment of plant (*Arabidopsis thaliana*) lipid transfer protein 4 (LTP4)—SpotReport mRNA spike 4 (Stratagene) was subjected to SMART amplification (Clontech), following the manufacturer's instructions, except for the 5'SMART oligonucleotide which was modified to carry the T7 RNA Polymerase promoter (T7-SWITCH primer). The full-length B2M, TBP and LTP4 fragment were cloned into a pCR 2.1-TOPO vector (Invitrogen). The constructs were sequenced and used in a new PCR to produce the corresponding amplicons, which were cleaned using a QIAquick PCR purification kit (Qiagen). The single band of amplification product was confirmed by running a 1.5% agarose gel containing ethidium bromide for visualization.

To generate standard calibration curves, 6-fold serial dilutions of corresponding amplicons were made on 50 ng/ μ l yeast tRNA as a carrier. The calibration curves have spanned \sim 4 orders of magnitude. The standards were kept at 4°C. To check the reproducibility of the standard calibration curve, the runs were carried out at least four times with the same standard dilutions in a time period of over a month, on different days.

RT reactions

For each reaction in a total volume of 20 μ l, 500 ng oligo (dT)₍₁₂₋₁₈₎, dNTP mix (0.5 mM each) and a corresponding

amount of either 50 ng or 1 μ g of total RNA (LN 229) were added. The total RNA dilution was made on yeast tRNA solution to introduce 100 ng of the carrier to the RT reaction. Each RT reaction was run in triplicate. The mixture was heated at 65°C for 5 min and incubated on ice for 3 min. The first strand buffer (50 mM Tris-HCl, pH 8.3, 75 mM KCl and 3 mM MgCl₂), 5 mM DTT and 5 U of RNase Inhibitor (Invitrogen) were added into each tube. The tubes were incubated at 42°C for 5 min, then 200 U of SuperScript III (Invitrogen) were added and tubes were incubated at 50°C for 40 min, 55°C for 20 min and 70°C for 15 min. Then, the cDNA:RNA hybrid was treated with 2 U of RNase H (Invitrogen) at 37°C for 20 min. The dilution solution of a carrier (50 ng/ μ l yeast tRNA—41.5 μ l) was added to each tube. The contents were mixed and split for two tubes; one tube was used for further phenol/chloroform/isoamyl alcohol (PCI) treatment followed by ethanol precipitation (PCI sample), and the second tube received no further purification (Figure 1).

Phenol/chloroform/isoamyl alcohol (PCI) procedure followed by ethanol precipitation

PCI samples (31.2 μ l) were subjected to organic extraction followed by EtOH precipitation. Linear Polyacrylamide (LPA), GenElute LPA (Sigma), 15 μ g (1 μ g/ μ l) was added to each sample before the PCI procedure, along with 1 \times TE, pH 8.0 (Sigma) to bring the final volume to 100 μ l. For extraction of cDNA, 100 μ l of PCI, pH 8.0 (Amresco) was added to each PCI sample. Samples were then vortexed for 1 min, allowed to stand for 5 min and then centrifuged at 7000 g for 5 min at room temperature. The procedure was carried out in safe-lock tubes (Eppendorf). The aqueous phase was slowly aspirated in a steady fashion and transferred into a new tube. Tris-EDTA, 1 \times , 100 μ l was added to the extraction tube and

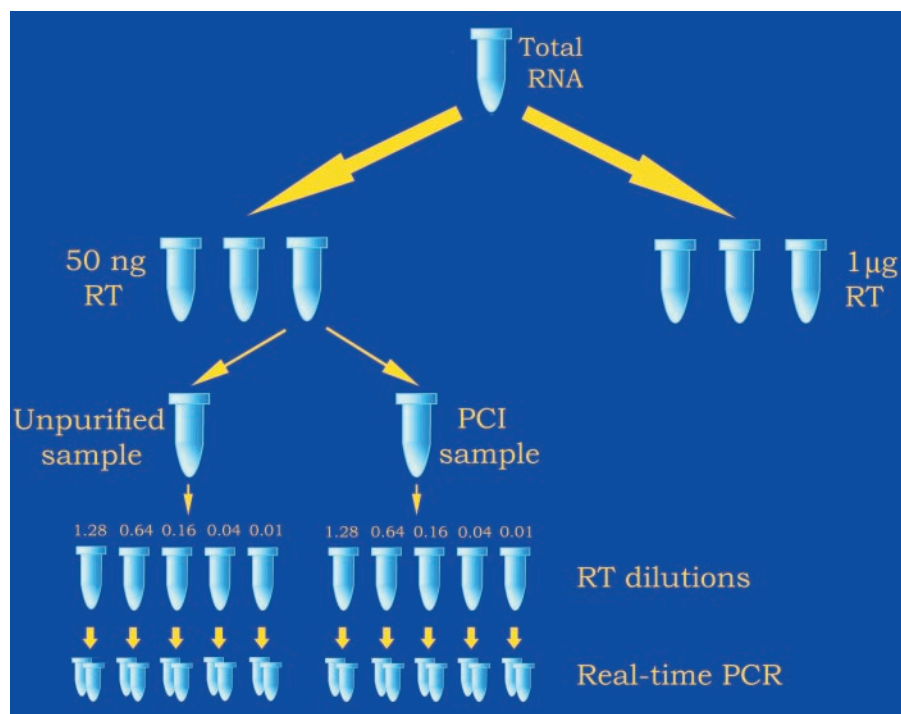


Figure 1. Experimental layout: comparison of unpurified and PCI samples.

the PCI procedure was repeated again, giving the final volume of ~200 μ l. We then added 1/10 vol of 5 M ammonium acetate (Ambion) and mixed thoroughly. Then, 2.6 vol of pre-chilled 96% Ethanol (Sigma) was added, mixed again, spun shortly and precipitated at -20°C overnight.

The next day the tubes were placed into a high-speed centrifuge pre-cooled to 4°C , and centrifuged at 15 000 g for 1 h. The pellet was thoroughly washed by 70% EtOH (1 ml) at room temperature. During this procedure the pellet was detached from the bottom of the tube and it was centrifuged once more at 15 000 g for 40 min at room temperature. The supernatant (EtOH and salts) was aspirated using 1 ml filtered pipette tip. The tube was spun down, and the rest of the ethanol was aspirated completely using sequentially 30 and 10 μ l filtered pipette tips without touching the pellet. The tubes were air dried for 3 min at room temperature, and 31.2 μ l of nuclease-free water was added. The contents were mixed, allowed to stand first for 15 min at room temperature and then either 1 h or overnight at 4°C before PCR.

PCR

PCRs were carried out either on 1 μ g or 50 ng RT reactions diluted as described above (first point) as well as on standards. To build a calibration curve for each sample, their contents were diluted twice with 50 ng/ μ l yeast tRNA (second point), and then 4-fold sequentially (points 3, 4 and 5). Real-time PCR was carried out in a 24 μ l reaction volume containing 1 \times SYBR Green PCR Master Mix (Applied Biosystems), 140 nM of each primer and 4 μ l of template dilution. The thermal profile for PCR was 95°C for 10 min, followed by 40 cycles of 95°C for 15 s and 60°C for 1 min. Data were collected using the 7700 SDS thermal cycler (Applied Biosystems). Each sample was run in duplicate. The melting curve was examined for each tube to confirm a single peak appearance. Minus RT reactions were set up also, and PCR negative controls were run for each pair of primers. In order to generate primer pairs, the full-length mRNA structure was converted as an antisense strand that corresponds to a first cDNA strand. The structure was analyzed using the Mfold program (9) to find the sequence with least complexity. The primers were designed using Oligo 6 (Molecular Biology Insights) and were synthesized either by Invitrogen or Sigma Genosys. Primer sequences are presented in Supplementary Table 1.

Detection of DNA synthesis activity of RT in PCR conditions

Two experimental sets were applied. The first set of experiments had two parts. Two RT reactions with 1 μ g of total RNA (LN229) were established and processed, as described above. One RT reaction was subjected to the PCI procedure, and another received no purification. For the first part of experiments, the amounts corresponding to 1.28 and 0.64 μ l of undiluted unpurified RT reaction were taken into PCR. The same volumes of unpurified RT reaction were accompanied with either 70 or 140 ng of total RNA (LN229). The real-time PCR was set up without *Taq* Polymerase using a SYBR Green PCR Core Kit (Applied Biosystems) as recommended by the manufacturer: 1 \times SYBR Green Buffer, 3 mM MgCl_2 , 0.2 mM of each dNTP and 140 mM of primers. For the second part of experiments, 51.2, 12.8 or 3.2 U of SuperScript III (SS III)

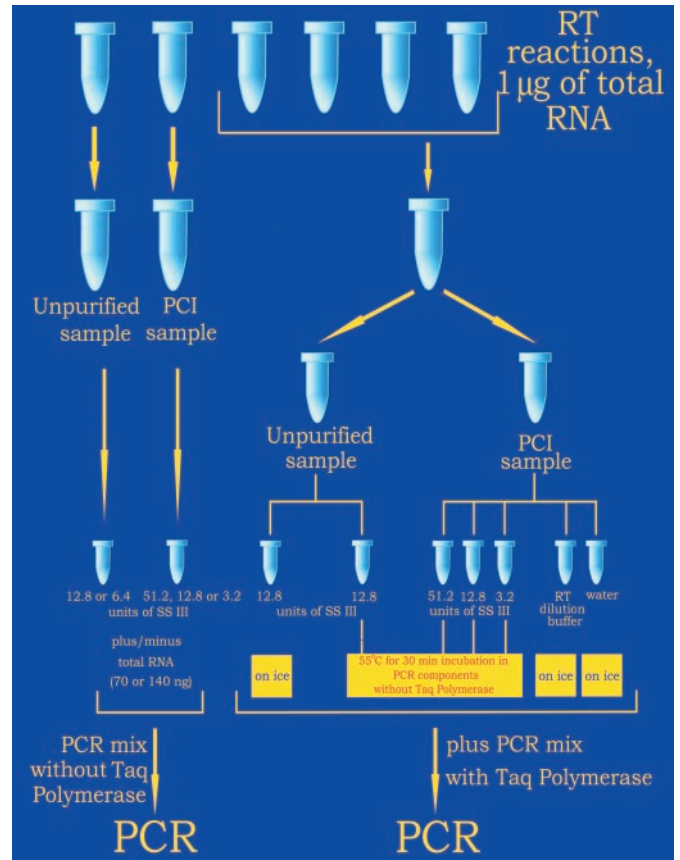


Figure 2. Experiments to detect DNA synthesis activity of RT.

were combined either with 4 μ l of diluted RT reaction after the PCI procedure or with total RNA (70 or 140 ng). The dilutions of SS III were made as recommended (10) on RT dilution buffer: 1 \times First Strand Buffer (Invitrogen) with 0.05% NP-40 (IGEPAL CA-630, Sigma) to protect RT activity. SYBR Green mix without *Taq* Polymerase was added to each tube to the final volume of 24 μ l (Figure 2).

The second set of experiments had two parts also. Four separate RT reactions with 1 μ g of total RNA (LN229) were performed and were diluted as described above. The contents of all tubes were combined together, giving a final volume of 250 μ l. We took 76 μ l of combined RT reactions without any purification step for the first part of the experiment and the rest of RT reaction product was split equally for two tubes (87 μ l each) which were purified using the PCI procedure followed by EtOH precipitation, as described above. The pellet was dissolved in 87 μ l of water and two tubes were combined and were taken for the second part of the experiment. For the first part of the experiment, 4 μ l of diluted unpurified RT reaction were combined with SYBR Green PCR Core Kit components without *Taq* Polymerase in a final volume of 24 μ l. The tubes were incubated at 55°C for 30 min, while the control set of tubes was kept on ice. For the second part of the experiment, 4 μ l of diluted purified RT reaction were taken into 24 μ l of a PCR without *Taq* Polymerase, but with 51.2, 12.8 or 3.2 U of SS III. The tubes were incubated at 55°C for 30 min. The control set of tubes, where SS III was substituted with RT dilution buffer, was kept on ice. All reactions were run in

quadruplicate. After incubation, 26 μ l of SYBR Green PCR Core Kit Master Mix with 1.25 U of AmpliTaq Gold Polymerase (Applied Biosystems) were added to both incubated and control sets of tubes and were then subjected to PCR runs with two pairs of primers, B2M and TBP (Figure 2).

RNA amplification experiment

Six reactions with 20 ng of total RNA (LN229) were set up for RNA amplification.

Total RNA was mixed with 0.5 μ l of 10 μ M modified oligo(dT) primer [5'-AGCAGTGGTAACAACGCTAATACG(T)₂₂-3'] and 0.5 μ l of 10 μ M T7-SWITCH oligonucleotide [5'-AGCAGTGGTAACAACGCTAATACGACTCACTATA-Gr(GGG)-3'] in 5 μ l of final volume. The tubes were incubated at 72°C for 2 min and then chilled on ice. The first strand buffer (25 mM Tris-HCl, pH 8.3, 37.5 mM KCl and 1.5 mM MgCl₂), 1 mM dNTP, 2 mM DTT (Invitrogen) and 3 mM MgCl₂ (Sigma) were added to each tube (all concentrations are final). The tubes were incubated at 42°C for 5 min, then 1 μ l of Superscript II (Invitrogen) was added, and the tubes were incubated at 42°C additionally for 1 h. The final volume of reaction was 10 μ l. Three out of six reactions were cleaned up by a PCI procedure followed by an EtOH precipitation as described above, and the other three RT reactions received no purification. The first-strand cDNA pool was then subjected to LD (Long Distance) amplification using the Advantage 2 PCR Enzyme System (CLONTECH) and amplification primer (5'-GCAGTGGTAACAACGCTAATACG-3') to produce double-stranded cDNA as recommended by the manufacturer. An MJR PCR machine was used for amplification with the following parameters: 95°C for 1 min; (95°C for 15 s, 65°C for 30 s, 68°C for 6 min)—12 cycles. The alkaline hydrolysis of RNA (7.5 μ l of 1 M NaOH, 2 mM EDTA at 65°C for 5 min) was followed by neutralization with 0.5 M Tris-HCl, pH 6.8 (12.5 μ l). The double-stranded DNA pool bearing T7 Promoter was purified using a QIAquick PCR Purification Kit (Qiagen) and concentrated on Microcon, YM-30 columns (Millipore) following the manufacturer's instructions. RNA was transcribed from double-stranded DNA using reagents from a MEGAScript High Yield Transcription Kit (Ambion). The mixture of double-stranded DNA (12 μ l), 12 μ l of 75 mM rNTP, 3 μ l of 10 \times Buffer and 3 μ l of Enzyme Mix (RNase Inhibitor and T7 RNA Polymerase) was incubated at 37°C for 18 h. Upon completion, the reactions were treated with 2 μ l of DNase I (Ambion) at 37°C for 30 min. The amplified sense RNA was purified using a MEGAclear Kit (Ambion) as described in the Ambion instruction manual. The RNA yield was evaluated by SmartSpec 3000 (BioRad).

Data analysis

Data were analyzed with 7700 SDS software (Version 1.9.1) and transferred to Excel. To retrieve C_t values the appropriate thresholds were set up as recommended [(11,12) and http://www.appliedbiosystems.com/support/tutorials/pdf/data_analysis_7700.pdf]. The slope was calculated from the plot of log transformation of serial dilution versus C_t (samples), or log transformation of initial target copy number versus C_t (standards). The amplification efficiency (E) was determined based on the slope of this graph as $E = 10^{(-1/\text{slope})}$. To assess the inhibitory effect for every dilution point of sample, the

initial input (number of molecules) was calculated based on the standard calibration curve for corresponding pairs of primers. The significance of difference between two groups was tested using a two-tailed t -test. The type of t -test was determined by calculating the variance ratio of two samples of comparison at $F \leq 0.05$.

RESULTS

To address the global nature of inhibitory effects of RT reaction components on PCR, we made RT reactions where 50 ng of total RNA was taken along with 100 ng of a carrier, yeast tRNA. All reactions were split equally for two tubes. The first tube of each RT reaction was subjected to the PCI procedure followed by the EtOH precipitation, while the second one received no further treatment. The dilutions of RT reactions were made in a way that the amount corresponding to 1.28 and 0.64 μ l of undiluted RT reaction was introduced into the PCR. Fourteen different primer pairs with different locations on the transcript's sequence (5' and 3' ends), and with different levels of expression were utilized for real-time PCR. Each primer pair was implemented for three different RT reactions. Because the dilution was 2-fold, the expected $\Delta C_t = C_{t,0.64} - C_{t,1.28}$ should be either equal to 1, when $E = 2$, or bigger than 1, when $E < 2$. In the meantime, ΔC_t values were < 0.6 for 5'-ACTB (β -actin), 5'-TFRC (transferring receptor), 5'-HPRT1 (hypoxanthine phosphoribosyltransferase 1), 3'-ENO2 (enolase 2, gamma, neuronal), 3'-ERP70 (protein disulfide isomerase related protein) and 3'-FAP (fibroblast activation protein, alpha). Moreover, ΔC_t values for 3'-ACTB, 3'-HPRT1, 3'-TNC (tenascin C), 5'-TNC, 3'-TFRC and 5'-B2M were even negative, meaning that C_t values of more diluted samples were lower than those of concentrated samples, and, theoretically, it should be the opposite. Only two out of fourteen pairs gave ΔC_t values close to 1: ΔC_t for 5'-ERP70 was 0.79 and ΔC_t for 3'-TBP was 0.9. In the meantime, ΔC_t values span a range of 0.85 – 1.24 when the PCI procedure followed by EtOH precipitation was utilized in these pilot experiments. The PCI samples always gave lower C_t values than their unpurified counterparts (Supplementary Table 2).

To explore how the inhibition of PCR affects the linearity within dilutions and the reproducibility across the identical samples, we made three RT reactions with 50 ng of total RNA (LN229) together with 100 ng of yeast tRNA as a carrier (50 ng RT). All reactions were equally divided in two tubes after RT reaction. The first tube of each pair was subjected to the PCI procedure followed by EtOH precipitation, while the second one received no further treatment (Figure 1). We used two primer pairs for real-time PCR. The first appears to be under moderate inhibition—B2M ($\Delta C_t = -0.05$), and the second, TBP ($\Delta C_t = 0.9$)—without any visible inhibition. These pairs were chosen for another reason: B2M gene expression level is moderate-high, and TBP is a relatively rarely expressed gene. Finally, these transcripts are often considered as candidates for reference genes in the normalization procedure (13).

Figure 3 shows that the variability was dramatically decreased when the PCI procedure was implemented, especially for the first two points for 50 ng RT reactions.

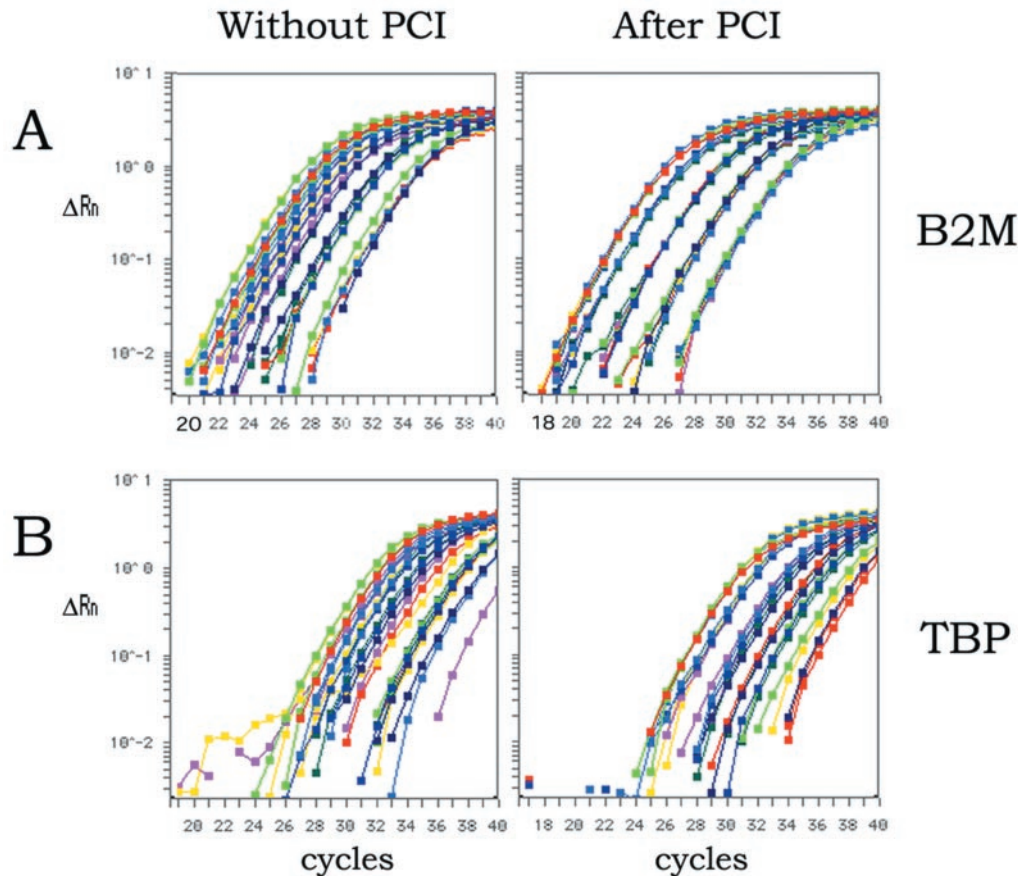


Figure 3. The PCI procedure improves the real-time PCR results, when 50 ng of total RNA was taken for RT reaction. The dilutions correspond to certain volumes of undiluted RT reaction—1.28, 0.64, 0.16, 0.04 and 0.01 μ l were used as a template in PCR with a B2M pair of primers (A) and a TBP pair of primers (B).

Mean C_t values, SD and coefficient of variability (CV) for every point of calibration curve are presented in Table 1, Block A. In general, C_t values for the PCI sample are lower than those for the unpurified sample. There is a decrease in SD and CV for PCI samples in every dilution point for both B2M and TBP pairs. The difference is statistically significant for every dilution point for a B2M pair ($P \leq 0.004$). It should also be mentioned that SD and CV of an unpurified sample with a B2M pair were improved with dilution (points 4 and 5). For TBP pairs the difference is also significant for the first two points with an increase of P -value for points 3 and 4. Finally, there is no significant difference at point 5 ($C_t > 34$), $P = 0.5588$ (Table 1, Block A). The high C_t value variability of unpurified samples leads to poor reproducibility. The ratio between three identical samples should be around 1 for every given point. This is the case when the PCI procedure was implemented. The ratio is in a range of 0.9–1.1 for every dilution point with a B2M pair (compare with unpurified sample—0.6–3.2), and the comparison of two first points for a TBP pair gave a ratio range of 0.9–1.2 (compare with unpurified sample—0.7–2.0).

To calculate the inhibitory effect for each dilution point, the C_t values were transformed into number of molecules using the corresponding standard calibration curve. The percentage of molecules in an unpurified sample, excluded from PCR, in comparison with the PCI sample was calculated by

the formula:

$$\text{Inhibitory percentage (IP)} = 100 - \left[\frac{\text{molecules in unpurified sample}}{\text{molecules in PCI sample}} \times 100 \right] \quad 1$$

Overall, it is possible to see a decrease in inhibition with every next dilution for a B2M pair in 50 ng RT. The IP values are also provided for a TBP pair for every dilution point, but it should be mentioned that only the first and the second points are in confident range, because of the simultaneous increase of variability in points 3, 4 and 5 for both unpurified and purified samples.

To understand how the amount of total RNA introduced in RT reactions affects the inhibitory processes, a similar experiment with the same range of dilution of RT reactions to that presented in Figure 3 (50 ng RT) was executed, except that in this case 20 times more RNA, 1 μ g, was taken for RT reactions (1 μ g RT). No visual inhibitory effect was observed (Supplementary Figure 1), though there is still a calculated IP (up to 30%) for every pair at each dilution point, except the first (Table 1, Block B). In general, SD and CV values of each point, except the first, were still lower for samples after the PCI procedure (1 μ g RT), but the statistical significance was decreased in comparison to 50 ng RT (Table 1, Blocks A and B). The C_t values of the first point of unpurified samples

were lower than those of PCI samples for both transcripts, and the difference is statistically significant ($P \leq 0.0094$). We repeated this experiment taking three new RT reactions for dilutions with one exception, 1× TE, pH 8.0 was substituted with 10 mM Tris, pH 8.0 for the PCI sample (data not shown). The lower C_t values of the first point for samples without purification versus those for PCI samples were confirmed.

We thought that this effect could result from DNA synthesis activity of RT, so we tried to detect it using two approaches (Figure 2). The direct one, when different amounts of RT were introduced in the absence of *Taq* Polymerase gave no visible amplification, regardless of which template was utilized (cDNA, total RNA or cDNA together with total RNA). We decided to use a two-step approach, since the residual DNA synthesis activity of RT might be visible only when amplified with *Taq* Polymerase. The first part of the experiment was run with unpurified RT reaction in the PCR components without *Taq* Polymerase. This set of tubes was subjected to an extra incubation at 55°C for 30 min, while the control set was kept on ice. The PCR components with *Taq* Polymerase were added afterwards. We did not observe any difference for a TBP pair. The average C_t value for tubes with extra incubation was 23.13 ± 0.03 in comparison with that of the control set: $C_t = 23.11 \pm 0.11$ with $P = 0.84$. The control set for a B2M pair has a slightly lower C_t value compared with that for tubes with extra incubation (17.13 ± 0.01 versus 17.21 ± 0.01 with $P = 0.0001$). It is noteworthy that the same amount of reverse transcriptase was used in both—control tubes and tubes with extra incubations. We were able to see more dramatic differences when the samples with RT were compared with samples without it. The different amounts of SS III were mixed with 4 µl of diluted RT reaction after the PCI procedure and PCR components in the absence of *Taq* Polymerase. These tubes were subjected to an extra incubation step at 55°C for 30 min, and the control set was kept on ice. The PCR components with *Taq* Polymerase were added to both sets, and PCR was executed in a final volume of 50 µl. The high concentrations of SS III (51.2 and 12.8 U) inhibited PCR with a B2M pair of primers (20.06 ± 0.34 versus 17.35 ± 0.07 for control set, $P = 0.0004$, and 17.75 ± 0.08 versus 17.35 ± 0.07 with $P = 0.0002$), while the average C_t value was slightly lower for tubes with 3.2 U of than that for controls without RT (17.22 ± 0.03 versus 17.35 ± 0.07 with $P = 0.014$). All concentrations of SS III caused the overamplification when a TBP pair of primers was utilized. The C_t value was 22.55 ± 0.12 for 51.2 U of RT, $C_t = 22.46 \pm 0.12$ for 12.8 U of RT and $C_t = 22.97 \pm 0.02$ for 3.2 U of RT in comparison with the control set without SS III, $C_t = 23.14 \pm 0.05$. The differences were statistically significant with corresponding P -values equal to 0.00008, 0.00004 and 0.001. To check any influence of RT dilution buffer with NP-40 on PCR, the control set of tubes was established with water substituted for the buffer. The C_t values were slightly lower for PCR tubes with RT dilution buffer than those with water for both pairs (17.35 ± 0.07 versus 17.42 ± 0.03 for a B2M pair, and 23.14 ± 0.05 versus 23.28 ± 0.08 for a TBP pair). One of the four negative controls of TBP pair was positive with $C_t = 37.71$.

Table 2 provides the comparison of efficiency of PCR amplification (E) and coefficient of correlation (R^2) derived from the slope of calibration curves for unpurified and PCI samples

Table 2. Amplification efficiency (E) and coefficient of correlation (R^2) derived from the slope of a sample's calibration curve

Sample name	50 ng for RT		#3-no PCI		#1-PCI	#2-PCI	#3-PCI	#4-no PCI		1 µg for RT		#4-PCI	#5-PCI	#6-PCI
	#1-no PCI	#2-no PCI	#3-no PCI	#1-PCI	#2-PCI	#3-PCI	#4-no PCI	#5-no PCI	#6-no PCI	#4-PCI	#5-PCI	#6-PCI	#5-PCI	#6-PCI
E/R^2 -5 points	(2.03/0.9798)	1.96/0.9906	(2.29/0.9662)	1.85/0.9989	1.82/0.9989	1.84/0.9987	1.77/0.9958	1.74/0.9968	1.77/0.9984	1.84/0.9991	1.86/0.9991	1.84/0.9984	1.86/0.994	1.88/0.9989
E/R^2 -4 points	(1.91/0.9893)	1.88/0.9919	2.08/0.9937	1.84/0.9984	1.81/0.9983	1.82/0.9986	1.81/0.9984	1.78/0.9982	1.80/0.9996	1.82/0.9991	1.83/0.9924	1.82/0.9991	1.83/0.9924	1.87/0.9983
$E_{\text{average-5}}$ points	na			1.84 ± 0.02/0.9991 ± 0.0003	1.84 ± 0.02/0.9988 ± 0.0001		1.76 ± 0.02/0.9970 ± 0.0013			1.86 ± 0.02/0.9973 ± 0.0029				
E/R^2 , Standard curve			1.85 ± 0.01/0.9991 ± 0.0003						1.85 ± 0.01/0.9991 ± 0.0003					

The B2M pair of primers was utilized for each, unpurified (no PCI) and purified (PCI) samples at the different RNA amounts for an RT reaction. The calibration curves were built either using all dilution points (E/R^2 -5 points) or by excluding the first, most concentrated dilution point (E/R^2 -4 points). The derived E values with $R^2 < 0.99$ are presented in the parentheses and in italic.

at different template levels for RT reactions (50 ng and 1 μ g) for a B2M pair. A similar table for a TBP pair is presented in the Supplementary Table 3. Since a noticeable inhibition occurs at the first point of unpurified samples, there is a poor linearity ($R^2 < 0.99$) within the calibration curves derived by plotting C_t values of five dilution points against log transformation of dilution (B2M pair, 50 ng RT). With the four points approach—excluding the first, most concentrated point—2 out of 3 plots with $R^2 > 0.99$ were built, and increased E -values as much as 2.08 were derived. The improved coefficients of correlation ($R^2 \geq 0.9987$) were associated with the calibration curves for PCI samples (B2M pair). We were unable to build the calibration curves for TBP with $R^2 \geq 0.99$ either for unpurified or PCI samples (50 ng RT), except in one case for the PCI sample (Supplementary Table 3). Most important, there is a similarity in amplification efficiencies between PCI samples and standard calibration curves for both 50 ng and 1 μ g RT reactions and E of unpurified samples are different from those of the standard calibration curve (Table 2). Note that when the four points approach was used for unpurified sample calibration curves for 1 μ g RT by excluding the first point, this leads to an increase of R^2 and E -values for both pairs, B2M and TBP (Table 2 and Supplementary Table 3).

We also compared the expression ratio between 1 μ g and 50 ng RT for both transcripts in all possible combinations with an expected value equal to 20. The average ratios for each calibration point of PCI sample for a B2M pair were 20 ± 1 , 21 ± 1 , 24 ± 1 , 28 ± 4 and 27 ± 2 . This should be compared with the unpurified sample: 145 ± 70 , 63 ± 22 , 44 ± 11 , 39 ± 8 and 42 ± 7 . When a TBP pair was used, PCI samples gave the following ratios: 19 ± 1 , 21 ± 3 , 22 ± 7 , 21 ± 6 and 19 ± 9 in comparison with those of unpurified sample: 61 ± 21 , 44 ± 12 , 30 ± 10 , 32 ± 12 and 21 ± 15 .

We compared two different purification systems of RT reactions: EtOH precipitation without the PCI step and a PCI procedure followed by an EtOH precipitation—the approach has been described above. Three RT reactions with 50 ng of total RNA (LN229) together with 100 ng of yeast tRNA as a carrier were equally divided in two tubes. Each tube of the pair was subjected to EtOH precipitation as already described, but a PCI procedure was implemented only for the second tube of the pair. We utilized TBP and B2M pairs for PCR. Mean C_t values were lower for PCI samples than those for samples after EtOH precipitation alone for both B2M and a TBP pairs (Supplementary Table 4). The difference is statistically significant

for the first and second dilution points for the TBP pair ($P \leq 0.002$), and for every dilution point for a B2M pair ($P \leq 0.001$). Although, it has to be pointed out that the variability was decreased even for samples after EtOH precipitation alone, when compared with unpurified samples (Supplementary Table 4 and Table 1). The samples after EtOH precipitation, when the PCI step was omitted, tend to exhibit artificially increased amplification efficiencies (2.01 and 2.08 for TBP pair; and 2.06 and 2.03 for B2M pair) as presented in Supplementary Table 5.

To evaluate how RT may influence other downstream applications other than RT-PCR, we performed an RNA amplification experiment. A yield of 22.4 ± 1.2 μ g of amplified RNA was generated from a starting amount of 20 ng of total RNA when RT reactions were cleaned up before double-strand DNA synthesis, compared with 1.1 ± 0.2 μ g of amplified RNA when the purification step was omitted.

The experiments were also performed in order to evaluate template loss during the PCI procedure followed by EtOH precipitation. We introduced double-stranded LTP amplicon after 50 ng RT reactions were completed. The added LTP amount corresponded to 15 molecules per cell, based on one cell containing 20 pg of total RNA, and 50 ng of total RNA corresponds to 2500 cells. The RT reactions with LTP spikes were split into two tubes, extracted and precipitated as described above. The control tube with the same amount of LTP amplicon but without any further treatment was used as a reference. The recovery percentage was 92.5 ± 4.8 . The experiments were carried out on three RT reactions in one experiment and were repeated on two different days.

Based on the finding from these experiments that the amplification efficiency could be more than 100% ($E > 2$), we performed a PCR simulation to understand whether the RT inhibition of PCR might cause the amplification efficiency overestimation.

The dilutions for the simulated calibration curve were assigned as follows: the first point corresponds to undiluted RT sample; the second point is a 2-fold dilution; and the third to seventh are sequential 4-fold dilutions. We assigned the IP values for first point as 90, 50 or 20%. The starting IP value was decreased in each 4-fold dilution with 30, 20 or 10% decrement (Table 3). The number of molecules competent for PCR in the first undiluted point was derived from the formula:

$$X_0 = X / (K_X \times E^{C_t, x}), \quad 2$$

Table 3. PCR simulation was made with different IP combinations—IP in the first point and the decrement

IP in 1st point (%)	The decrement (%)	Assigned $E = 2$			Assigned $E = 1.8$		
		E/R^2 , all points	E/R^2 , w/o 1st point	E/R^2 , w/o points 1, 2	E/R^2 , all points	E/R^2 , w/o 1st point	E/R^2 , w/o points 1, 2
90	30	<i>(2.59/0.9541)</i>	<i>(2.34/0.9821)</i>	2.16/0.9947	<i>(2.24/0.9541)</i>	<i>(2.05/0.9821)</i>	1.92/0.9947
	20	<i>(2.65/0.976)</i>	<i>(2.46/0.9894)</i>	2.30/0.9958	<i>(2.28/0.976)</i>	<i>(2.14/0.9894)</i>	2.03/0.9958
	10	2.48/0.994	2.39/0.997	2.31/0.9992	2.16/0.994	2.09/0.997	2.03/0.9992
50	30	2.12/0.9957	2.07/0.9976	2.01/0.9999	1.89/0.9957	1.85/0.9976	1.81/0.9999
	20	2.14/0.9969	2.10/0.9975	2.05/0.9989	1.91/0.9969	1.88/0.9975	1.84/0.9989
	10	2.15/0.9998	2.14/0.9998	2.12/0.9998	1.91/0.9998	1.90/0.9998	1.89/0.9998
	30	2.03/0.9995	2.01/1	2.00/1	1.82/0.9995	1.81/1	1.80/1
20	20	2.03/0.9996	2.02/0.9998	2.00/1	1.82/0.9996	1.81/0.9998	1.80/1
	10	2.04/0.9997	2.03/0.9997	2.01/0.9999	1.83/0.9997	1.82/0.9997	1.81/0.9999

The derived E values with $R^2 < 0.99$ are presented in the parentheses and in italic.

where

$$K_X = (100 - IP_{X_0})/100, \quad 3$$

X_0 is starting concentration, X is amount of product after $C_{t,x}$ cycles, and K_X is the inhibitory coefficient at this point. We established the amplification efficiency as $E = 1 + E'$ to simplify the presentation of formulae.

Then the number of molecules, PCR available in the second point (2-fold dilution) was defined by the formula:

$$Y_0 = Y/(K_Y \times E^{C_{t,y}}), \quad 4$$

where

$$K_Y = (100 - IP_{Y_0})/100, \quad 5$$

and

$$IP_{Y_0} = IP_{X_0} - \text{decrement}/2, \quad 6$$

since the decrement was assigned to a 4-fold dilution.

When $X = Y$ at the certain threshold, and $C_{t,x}$ is also assigned, it is possible to retrieve $C_{t,y}$ using the following equations:

$$X_0/Y_0 = (K_X \times E^{C_{t,y}})/(K_Y \times E^{C_{t,x}}) \quad 7$$

$$E^{(C_{t,y}-C_{t,x})} = (K_X \times X_0)/(K_Y \times Y_0) \quad 8$$

Equation 8 was converted by taking a logarithm of both sides:

$$(C_{t,y} - C_{t,x}) \times \log_E E = \log_E [(K_X \times X_0)/(K_Y \times Y_0)] \quad 9$$

$$C_{t,y} = \log_E [(K_X \times X_0)/(K_Y \times Y_0)] + C_{t,x}. \quad 10$$

Because we analyzed the PCR dynamics at two different amplification efficiencies, either binary logarithm was applied at $E = 2$ or the logarithm base value was 1.8 at $E = 1.8$.

Using this formula (Equation 10) we may calculate C_t values in every dilution point with every IP combination—IP in the first point plus any decrement. For example, if the number of molecules in the first point introduced into simulated PCR is 200 000 and IP value at this point is 90%, the number of competent molecules for PCR is defined by a formula: $K_X \times X_0 = 0.1 \times 200\,000 = 20\,000$. The number of molecules participating in PCR for the second, 2-fold dilution point was calculated as follows: $K_Y \times Y_0 = \{[100 - (90 - 30/2)]/100\} \times 100\,000 = 25\,000$, when the inhibitory decrement is 30%. When $C_{t,x}$ value is assigned as 21, $C_{t,y} = \log_E(20\,000/25\,000) + 21 = 20.69$ if $E = 2$. This example shows from theoretical a standpoint how more diluted samples may exhibit lower C_t values than those for undiluted ones.

The derived amplification efficiencies and coefficients of correlation are presented in Table 3. Several tendencies were observed. The coefficients of correlation were increased when most concentrated points under the biggest inhibitory influence were excluded from the calibration curve. When low starting IP = 20% was taken, the estimated efficiencies are almost identical to assigned ones with the acceptable linearity. It is possible to retrieve a correct E even at the moderate inhibition— $E = 50\%$ with a certain decrement (30%). The higher the starting IP at the first point the lower the possibility

to detect correct amplification efficiency, even after excluding the most concentrated points (see IP = 90% with all decrements). Interesting, the linearity could be acceptable ($R^2 \geq 0.994$) for IP = 90% with a 10% decrement even when all points were taken to build the calibration curve. The actual starting number of molecules is irrelevant for the determination of the slope of the calibration curve in this PCR simulation, but in a real experiment the increased variability at $C_t > 30$ may introduce the additional bias to E and R^2 , when the calibration curve is derived for rarely expressed transcripts.

DISCUSSION

It is acknowledged that the efficiency calculation from the slope of a calibration curve often overestimates PCR efficiency (14). At the same time, it is not unusual to see the derived PCR amplification efficiency exceeds 100%. We have observed this in our experiments, and it has been reported by others (8,15,16). This seems a bit paradoxical, and likewise is the finding of an overestimated efficiency in samples containing PCR inhibitors. Such a paradox could be reconciled by considering PCR competent molecules as an increasing percentage of the total molecules in a PCR tube with each sequential dilution.

What could be a possible mechanism of PCR inhibition by RT reaction components? It seems that a key factor is reverse transcriptase itself (3–5), in spite of minor potential influences by other RT reaction components (5,8). Reverse transcriptase may exhibit several activities:

- (i) RNA-dependent DNA polymerase activity (RT activity) (17,18);
- (ii) DNA-dependent DNA polymerase activity (19–24);
- (iii) terminal nucleotidyl transferase-like activity (TdT), or non-template directed nucleotide addition (10,25);
- (iv) RNase H activity, if the reverse transcriptase construct was not mutated to remove it;
- (v) strand transfer and displacement ability (26–28); and
- (vi) binding capacity.

A previous study has suggested that RT inhibition of PCR is mediated through direct interaction with a specific primer-template combination (4). The reverse transcriptase molecules may withstand the high temperatures and still retain their activities when bound to any primer-template complex as RNA:DNA, DNA:DNA or RNA:RNA (4,29,30). Also, the mutated MMLV, H⁻, SuperScript III has improved the enzyme's intrinsic thermal stability, and some of its activities could be preserved even without nucleic acid complex presence (10). Based on these observations, it is reasonable to propose that the fraction of molecules which was bound to nucleic acid complexes before the high temperature was applied (70°C, 15 min and 95°C, 10 min in our experiments) may retain a binding capacity as well as DNA polymerase activity—RNA- and/or DNA-dependent. RT molecules which were not bound to such a complexes may have dramatically reduced DNA synthesis capabilities, or no such an activity at all, while possessing the binding ability during post RT step manipulations. We suggest that the binding ability would be preserved up to 10 PCR cycles, and DNA synthesis activity

may be exhibited only during a few (1–3) PCR cycles, and also during a short stage (~2 min) before the first step of PCR when the temperature rises from 22°C to 95°C and *Taq* Polymerase molecules are not yet active.

We were unable to demonstrate DNA polymerase activity in an experiment where *Taq* Polymerase was substituted with RT, but if such activity is retained during a few cycles, the signal would be undetectable and possibly lost in background. Meanwhile, when the outcomes of RT activities were amplified by *Taq* Polymerase we detected DNA synthesis activity of RT (3.2 U) for a B2M pair, and for a TBP pair at any amount of RT. The effects we observed in our experiments could be explained by differential residual DNA polymerase activity and binding capacity of two RT fractions, free and bound. We believe there are two RT activities with opposite vectors: (i) RT amplifies the template that would lead to an overestimation of the number of molecules; and (ii) molecules of RT compete for binding sites with *Taq* Polymerase molecules, decreasing the amount of template to be detected. The inhibition in every dilution of RT sample is influenced by the RT/*Taq* Polymerase ratio (1,4). This ratio decreases with each sequential dilution, which also causes a decrease in inhibition.

The bound fraction of RT molecules is 20 times larger when 1 µg of RNA is taken into the RT reaction, when compared with that for 50 ng RT. The amount of template may also influence the longevity of DNA synthesis activity and the processivity of RT, and, again, there is 20 times more template in any dilution point of comparison between 1 µg RT and 50 ng RT. As a result, all described effects are driven mostly by inhibition, and the DNA polymerase activity is not dominant at a 50 ng RNA level, but DNA synthesis ability could be more profound when 1 µg of RNA is taken.

We detected an overestimation of the number of molecules for the first, most concentrated point of unpurified sample (1 µg RT) compared with that of the PCI sample for both TBP and B2M pairs with single band detection on a gel and a single peak of melting curve presence. Because we cannot rule out the possibility that this effect is tied to our purification system, we repeated the experiment, excluding EDTA, since it could chelate Mg²⁺ and affect PCR. Still, the results were confirmed. We also examined whether LPA may introduce such a bias by the inhibiting PCR at high concentrations. No such effect was detected. When the first point of unpurified sample was excluded from the calibration curve, the linearity was improved for both pairs, B2M and TBP, while there was no effect on linearity by the same approach for the PCI sample. Finally, a comparison of ratios (1 µg RT and 50 ng RT) between unpurified and PCI samples showed that the results were superior when the PCI step was introduced. These facts allow us to assume that the overestimation of number of molecules in the first point could be ascribed to an effect of unpurified sample, and it was probably caused by DNA polymerase activity of RT. Even though the IP should be highest at this point when compared with that of other dilution points, the DNA polymerase activity appears to be highest also. It could be the case that DNA synthesis activity surpasses the inhibition in this particular dilution point.

If we assume that the DNA synthesis activity drops faster than the inhibition with every next dilution, this might also explain the slight rise of IP for 1 µg RT. MMLV, H⁻ is an

enzyme with low processivity (20–60 nt), which could be influenced by template concentration (10,29). It means that 2–5 molecules of RT could be required to create a complementary strand of 100 bp amplicon. In fact, this number could be even larger. This is predetermined by the nature of amplification with a pair of specific primers. Only one-fourth of molecules after two PCR cycles have the target amplicon size, and other molecules are extended beyond the amplicon borders. As a result, even a 2-fold dilution may decrease DNA synthesis activity several times, when the inhibition defined by binding capacity may be decreased by only 10–20%.

To add a degree of complication to this interpretation, we may also assume that the binding affinities of free and bound RT fractions are different. Moreover, the binding capacity of both fractions may decrease with unknown dynamics during PCR. Whether or not RT directly interacts with *Taq* Polymerase is also an open question (1,4).

The DNA synthesis activity and binding capacity of RT molecules may be influenced by numerous factors. Apparently, the resulting amplification/inhibition effects could be different, depending upon what type of reverse transcriptase is utilized. For example, the internal stability of SuperScript III (MMLV, H⁻) is much higher than that of SuperScript II (MMLV, H⁻). The half-life of Superscript III is 220 min versus 6 min for SuperScript II at 50°C (10). AMV, H⁻ RT binds not only nucleic acid duplexes, but also single-stranded RNA (29), and this may explain why the introduction of non-homologous RNA relieves the inhibition for this particular type of RT (1), but it has no effect on MMLV, H⁻ RT (4). The type of RT-PCR (coupled or uncoupled) and its conditions will also influence the final results. Post-RT and pre-PCR handling of diluted RT samples, including an extra PCR step (uracil-DNA glycosylase treatment) and excluding RNase H treatment after the RT step, all together will affect the final outcome. For instance, RNase H not only degrades RNA in RNA:DNA duplexes, making primer binding sites readily available (31), but it also creates additional RT binding sites. The different types of priming during an RT reaction [(random, specific or oligo(dT))] may change the bound/free ratio of two RT fractions, which will affect the final results even apart from the fact that additional amplification of certain transcripts may occur with random priming during RT, due to the displacement process (28,32). Obviously, various specific pairs of primers taken for PCR will be under different levels of inhibition even within the same transcript, since the primer-template structure strongly influences RT binding affinity (33). This could explain the different levels of inhibition seen for different sets of primers. It has also been shown that RT promotes the accumulation of primer-dimers by adding nucleotides to the 3' end of primers (3).

All of this argues strongly in favor for removing reverse transcriptase molecules before performing real-time PCR. The method of purification we present here could be considered to be a universal equalizer, regardless of what RT type and conditions are implemented before PCR. We introduced the organic extraction step (34) before ethanol precipitation, because the proteins could be copurified if ethanol precipitation alone is utilized (35). The PCI treatment may have additional benefits, such as removing RNA from RNA:DNA

complexes and resolving some cDNA secondary structure complications. Implementation of the described approach leads to an improvement of real-time PCR results. Variability is decreased and the precision of detection is increased when a PCI procedure followed by ethanol precipitation is applied. When undiluted RT reactions starting with nanograms of total RNA are taken into PCR without purification, the inhibitory effects will be at their maxima. To decrease these effects, an investigator usually dilutes the RT reaction before PCR, but the resulting C_t values will be in an area with increased variability, low reproducibility and inconsistent detection (12,36,37). Our approach allows for template concentration by eliminating PCR inhibitors, which would be especially valuable in the detection of rarely expressed transcripts, or in clinical and environmental screening applications.

The applicability of the described method of purification goes beyond RT-PCR. It is reasonable to expect that reverse transcriptase may also affect other downstream applications, e.g. for RNA amplification where minute amounts of RNA are taken. The RT reaction usually is diluted only 5–6 times before introduction, without any purification, to the double-strand DNA synthesis reaction. The RT molecules may compete with DNA polymerase I under these conditions, thus decreasing the reaction efficiency. When we applied a PCI step in our amplification method (SMART-like + IVT), the yield of amplified RNA was increased more than 20 times. It must be pointed out that only ethanol precipitation could be utilized for methods based on the classical Eberwine approach (38), since it requires RNA priming for DNA synthesis. Indeed, the purification step was successfully implemented in this case after RT reaction (39) and after double-strand DNA synthesis (40).

In conclusion, the purification method described here is robust, reproducible, and provides a reliable recovery. It is also rather routine and even has the reputation of being easy to perform, but it does require some degree of familiarization dealing with an almost invisible pellet. There are, however, colored carriers and phase-lock tubes available that can simplify the procedure. Care should still be taken to ensure that the carrier's dye is not fluorescent, as it may interfere with real-time PCR. The introduction of a foreign reference DNA after the RT reaction is completed could afford monitoring of the recovery in each tube. The methodology described here has applicability in molecular phenotyping of valuable cell populations where small amounts of template, as in the case of studying different stem and progenitor cell populations (41), pose problems in the precise identification of genes and rare genes involved in normal and abnormal histogenetic events.

SUPPLEMENTARY DATA

Supplementary Data are available at NAR Online.

ACKNOWLEDGEMENTS

The authors thank Eric Laywell and Li Liu for critical reading of the manuscript, and Rudolph Spangler for providing the Sevag *et al.* paper. The authors also thank Tatyana Ignatova for providing the LN229 cell line, and Vadim Gornostaev and

Olga Tchigrinova for providing technical assistance with cell cultures. This work was supported by NIH/NINDS grant NS37556 and NIH/NHLBI grant HL 70143 to D.A.S. O.S. and D.A.S. also are involved with a biotechnology start-up company, RegenMed, Inc., that is focused on cell and molecular therapies that rely on stem cell and regenerative medicine technologies. Funding to pay the Open Access publication charges for this article was provided by NIH/NINDS grant NS37556.

Conflict of interest statement. None declared.

REFERENCES

- Sellner, L.N., Coelen, R.J. and Mackenzie, J.S. (1992) Reverse transcriptase inhibits *Taq* polymerase activity. *Nucleic Acids Res.*, **20**, 1487–1490.
- Fehlmann, C., Krapf, R. and Solioz, M. (1993) Reverse transcriptase can block polymerase chain reaction. *Clin. Chem.*, **39**, 368–369.
- Chumakov, K.M. (1994) Reverse transcriptase can inhibit PCR and stimulate primer-dimer formation. *PCR Methods Appl.*, **4**, 62–64.
- Chandler, D.P., Wagon, C.A. and Bolton, H., Jr (1998) Reverse transcriptase (RT) inhibition of PCR at low concentrations of template and its implications for quantitative RT-PCR. *Appl. Environ. Microbiol.*, **64**, 669–677.
- Liss, B. (2002) Improved quantitative real-time RT-PCR for expression profiling of individual cells. *Nucleic Acids Res.*, **30**, e89.
- Aatsinki, J.T., Lakkakorpi, J.T., Pietila, E.M. and Rajaniemi, H.J. (1994) A coupled one-step reverse transcription PCR procedure for generation of full-length open reading frames. *Biotechniques*, **16**, 282–284, 286–288.
- Karsai, A., Muller, S., Platz, S. and Hauser, M.T. (2002) Evaluation of a homemade SYBR green I reaction mixture for real-time PCR quantification of gene expression. *Biotechniques*, **232**, 790–792, 794–796.
- Deprez, R.H.L., Fijnvandraat, A.C., Ruijter, J.M. and Moorman, A.F.M. (2002) Sensitivity and accuracy of quantitative real-time polymerase chain reaction using SYBR green I depends on cDNA synthesis conditions. *Anal. Biochem.*, **307**, 63–69.
- Zuker, M. (2003) Mfold web server for nucleic acid folding and hybridization prediction. *Nucleic Acids Res.*, **31**, 3406–3415.
- Potter, J., Zheng, W. and Lee, J. (2003) Thermal stability and cDNA synthesis capability of SuperScript III reverse transcriptase. *Focus*, **25.1**, 19–24.
- Bar, T., Stahlberg, A., Muszta, A. and Kubista, M. (2003) Kinetic Outlier Detection (KOD) in real-time PCR. *Nucleic Acids Res.*, **31**, e105.
- Bustin, S.A. and Nolan, T. (2004) Pitfalls of quantitative real-time reverse-transcription polymerase chain reaction. *J. Biomol. Tech.*, **15**, 155–166.
- Vandesompele, J., De Preter, K., Pattyn, F., Poppe, B., Van Roy, N., De Paep, A. and Speleman, F. (2002) Accurate normalization of real-time quantitative RT-PCR data by geometric averaging of multiple internal control genes. *Genome Biol.*, **18**, RESEARCH 0034. Epub.
- Pfaffl, M.W. (2004) Quantification strategies in real-time PCR. In Bustin, S.A. (ed.), *A-Z of Quantitative PCR*. International University Line, La Jolla, California, p.103.
- Pfaffl, M.W. (2001) A new mathematical model for relative quantification in real-time RT-PCR. *Nucleic Acids Res.*, **29**, e45.
- Peters, I.R., Helps, C.R., Hall, E.J. and Day, M.J. (2004) Real-time RT-PCR: considerations for efficient and sensitive assay design. *J. Immunol. Methods*, **286**, 203–217.
- Baltimore, D. (1970) RNA-dependent DNA polymerase in virions of RNA tumour viruses. *Nature*, **226**, 1209–1211.
- Temin, H.M. and Mizutani, S. (1970) RNA-dependent DNA polymerase in virions of Rous sarcoma virus. *Nature*, **226**, 1211–1213.
- Spiegelman, S., Burny, A., Das, M.R., Keydar, J., Schlom, J., Travnicek, M. and Watson, K. (1970) DNA-directed DNA polymerase activity in oncogenic RNA viruses. *Nature*, **227**, 1029–1031.
- Spiegelman, S., Burny, A., Das, M.R., Keydar, J., Schlom, J., Travnicek, M. and Watson, K. (1970) Synthetic DNA-RNA hybrids and RNA-RNA duplexes as templates for the polymerases of the oncogenic RNA viruses. *Nature*, **228**, 430–432.

21. Mizutani, S., Boettiger, D. and Temin, H.M. (1970) A DNA-dependent DNA polymerase and a DNA endonuclease in virions of Rous sarcoma virus. *Nature*, **228**, 424–427.
22. Myers, J.C., Dobkin, C. and Spiegelman, S. (1980) RNA primer used in synthesis of anticomplementary DNA by reverse transcriptase of avian myeloblastosis virus. *Proc. Natl Acad. Sci. USA*, **771**, 316–320.
23. Gao, G., Orlova, M., Georgiadis, M.M., Hendrickson, W.A. and Goff, S.P. (1997) Conferring RNA polymerase activity to a DNA polymerase: a single residue in reverse transcriptase controls substrate selection. *Proc. Natl Acad. Sci. USA*, **94**, 407–411.
24. Fisher, T.S., Darden, T. and Prasad, V.R. (2003) Mutations proximal to the minor groove-binding track of human immunodeficiency virus type 1 reverse transcriptase differentially affect utilization of RNA versus DNA as template. *J Virol.*, **77**, 5837–5845.
25. Chen, D. and Patton, J.T. (2001) Reverse transcriptase adds nontemplated nucleotides to cDNAs during 5'-RACE and primer extension. *Biotechniques*, **30**, 574–580, 582.
26. Fuentes, G.M., Fay, P.J. and Bambara, R.A. (1996) Relationship between plus strand DNA synthesis removal of downstream segments of RNA by human immunodeficiency virus, murine leukemia virus and avian myeloblastoma virus reverse transcriptases. *Nucleic Acids Res.*, **24**, 1719–1726.
27. Kulpa, D., Topping, R. and Telesnitsky, A. (1997) Determination of the site of first strand transfer during Moloney murine leukemia virus reverse transcription and identification of strand transfer-associated reverse transcriptase errors. *EMBO J.*, **16**, 856–865.
28. Nycz, C.M., Dean, C.H., Haaland, P.D., Spargo, C.A. and Walker, G.T. (1998) Quantitative reverse transcription strand displacement amplification: quantitation of nucleic acids using an isothermal amplification technique. *Anal. Biochem.*, **259**, 226–234.
29. Gerard, G.F., Potter, R.J., Smith, M.D., Rosenthal, K., Dhariwal, G., Lee, J. and Chatterjee, D.K. (2002) The role of template-primer in protection of reverse transcriptase from thermal inactivation. *Nucleic Acids Res.*, **30**, 3118–3129.
30. Mallet, F., Oriol, G., Mary, C., Verrier, B. and Mandrand, B. (1995) Continuous RT-PCR using AMV-RT and *Taq* DNA polymerase: characterization and comparison to uncoupled procedures. *Biotechniques*, **18**, 678–687.
31. Polumuri, S.K., Ruknudin, A. and Schulze, D.H. (2002) RNase H and its effects on PCR. *Biotechniques*, **32**, 1224–1225.
32. Zhang, J. and Byrne, C.D. (1999) Differential priming of RNA templates during cDNA synthesis markedly affects both accuracy and reproducibility of quantitative competitive reverse-transcriptase PCR. *Biochem. J.*, **337**, 231–241.
33. Schultz, S.J., Zhang, M., Kelleher, C.D. and Champoux, J.J. (1999) Polypurine tract primer generation and utilization by Moloney murine leukemia virus reverse transcriptase. *J. Biol. Chem.*, **274**, 34547–34555.
34. Sevag, M.G., Lackman, D.B. and Smolens, J. (1938) The isolation of the components of streptococcal nucleoproteins in serologically active form. *Streptococcal Nucleoproteins*, 425–436.
35. England, S. and Seifter, S. (1990) Precipitation Techniques. In Deutscher, M.P. (ed.), *Guide to Protein Purification. Methods in Enzymology*. Academic Press, INC, San Diego, CA, pp. 296–298.
36. Stahlberg, A., Hakansson, J., Xian, X., Semb, H. and Kubista, M. (2004) Properties of the reverse transcription reaction in mRNA quantification. *Clin. Chem.*, **50**, 509–515. Epub.
37. Soong, R. and Ladanyi, A. (2003) Improved indicators for assessing the reliability of detection and quantification by kinetic PCR. *Clin. Chem.*, **49**, 973–976.
38. Van Gelder, R.N., von Zastrow, M.E., Yool, A., Dement, W.C., Barchas, J.D. and Eberwine, J.H. (1990) Amplified RNA synthesized from limited quantities of heterogeneous cDNA. *Proc. Natl Acad. Sci. USA*, **87**, 1663–1667.
39. Wang, Q.T., Xiao, W., Mindrinos, M. and Davis, R.W. (2002) Yeast tRNA as carrier in the isolation of microscale RNA for global amplification and expression profiling. *Biotechniques*, **33**, 788, 790, 792 passim.
40. Naderi, A., Ahmed, A.A., Barbosa-Morais, N.L., Aparicio, S., Brenton, J.D. and Caldas, C. (2004) Expression microarray reproducibility is improved by optimising purification steps in RNA amplification and labelling. *BMC Genomics*, **5**, 9.
41. Suslov, O.N., Kukekov, V.G., Ignatova, T.N. and Steindler, D.A. (2002) Neural stem cell heterogeneity demonstrated by molecular phenotyping of clonal neurospheres. *Proc. Natl Acad. Sci. USA*, **99**, 14506–14511. Epub.